HEFAT2010
7th International Conference on Heat Transfer, Fluid Mechanics and Thermodynamics
19-21 July 2010
Antalya, Turkey

SIMULATION OF BLOOD FLOW IN HUMAN AORTA FOR EXTRACORPORAL CIRCULATION

[1]Benim A.C*, [1]Gul, F., [1]Nahavandi, A., [2]Assmann, A, [2]Feindt, P. and [3]Joos, F.
*Author for correspondence
[1]Department of Mechanical and Process Engineering,
Duesseldorf University of Applied Sciences,
Josef-Gockeln-Str. 9, D-40474 Duesseldorf,
Germany,
E-mail: alicemal.benim@fh-duesseldorf.de
[2]Department of Thoracic and Cardiovascular Surgery,
University Hospital,
Moorenstr. 5, D-40225 Duesseldorf,
Germany,
[3]Laboratory of Turbomachinery,
Helmut Schmidt University,
Holstenhofweg 85, D-22043 Hamburg
Germany.

ABSTRACT

Extracorporeal circulation is a standard technique in cardiovascular surgery, which can be applied in different variations. Using computational fluid dynamics, the impact of a particular perfusion technique for a certain patient can be simulated preoperatively, by considering the patient-specific physiology. By the developed procedure, the real geometry of the aorta of an individual patient can be captured and analyzed. The pulsatile and steady-state physiological blood flow, as well as the antegrade perfusion are computationally investigated for a patient, who exhibits some anomalies in the aorta physiology. The same flow configurations are investigated for a rather idealized aorta, without any apparent anomaly. The results are compared. It is demonstrated that the consequences of the antegrade perfusion for an abnormal and idealized/normal aorta turn out to be different, depending on the details of the aorta physiology. This comparison indicates that it is advisable to perform a patient-specific detailed computational analysis in advance, for the patients with abnormal physiology, instead of assuming a normal behavior for extracorporeal circulation.

INTRODUCTION

Biofluid dynamics that combines engineering with medical research is a rather new and a strongly expanding field of science [1]. Although other flows, such as the air flow in the pulmonary system [2] are also being considered within this scope, the dynamics of the blood flow stay very much in the foreground [3], which is also the subject of the present study. Particularly, the blood flow in human aorta is of present interest, with emphasis on extracorporeal circulation [4].

In the area of developing artificial heart valves or circulatory assist devices a rather large amount of investigations has been performed [5, 6]. But a comparably less number of studies investigated the details of the aortic flow, especially in the context of extracorporeal circulation. Wood et al. [7] compared the data of aortic magnetic resonance imaging with the results of numerical simulation. A further numerical study with emphasis on the determination of physiological wall shear stress and blood flow profiles in the abdominal aorta was performed by Lee and Chen [8]. To the authors' opinion, with respect to the influence of extracorporeal circulation on the aortic flow field, there is still a lack in simulation and/or experimental studies.

Tokuda et al. [9] performed a finite element simulation of the antegrade perfusion of the ascending aorta during cardiopulmonary bypass. They detected "turbulences" in the aortic arch, which play an important role in the delamination and sequential embolization of arteriosclerotic plaques. However, although they referred to the phenomena of "turbulence", they did not give any hint about, if any and which turbulence model was used. Minakawa et al. [10] investigated retrograde perfusion via the axillary artery, but did not perform any numerical simulations. By means of particle image velocimetry, they found very high flow velocities and turbulence intensities in the ascending aorta, respectively the aortic arch.

To the best of the authors' knowledge, comparative scientific analysis of the impact of different types of extracorporeal circulation on the aortic flow patterns, and especially on the aortic wall shear stress profile has not been performed yet, except for a recent investigation of the present authors [11], where both antegrade and retrograde perfusion techniques were numerically analysed by Computational Fluid Dynamics (CFD) and compared with each other. In that study, the analysis was based on an idealized aorta geometry.

The current analysis represents an improvement of that work, where the real aorta geometry of an individual patient is captured, represented and analyzed. Pulsatile and steady-state physiological circulation as well as steady-state extracorporeal circulation with antegrade perfusion are considered. The considered real aorta physiology exhibits some anomalies. The results are compared with the predictions for an idealized aorta. Thus, conclusions are drawn for the application of antegrade perfusion for abnormal aorta geometries, in comparison to the normal physiological constitution.

MODELLING

Geometry Capturing, Boundaries, Grid Generation

In capturing the aorta geometry of an individual patient, the starting point of the analysis has been the Magnetic Resonance Tomography (MRT) data stored according to DICOM standards [12]. By means of open source software 3D Slicer [13] and Bioimage Suite [14], as well as with the help of an in-house developed interface program, the geometry data is imported in the Fluent's grid generator Gambit [15], where the grid is generated for subsequent flow analysis using the CFD solver Fluent [15]. The geometry of the idealized aorta is principally based on the data obtained on a healthy person. In that case, the idealized geometry is directly generated within the grid generator Gambit [15].

For each of the both aorta physiologies, two different geometry models are generated, one for modeling the physiological circulation, considering the basic aorta geometry, and one for modeling the extracorporeal circulation by an antegrade perfusion, considering the insertion of the cannula into the aorta. In the following, the idealized aorta geometry will be denoted by "Aorta-1", whereas the real aorta geometry of an individual patient exhibiting an aortic isthmus stenosis will be denoted by "Aorta-2".

Geometries of Aorta-1 and Aorta-2, for the case of antegrade perfusion (including the inserted cannula) are shown in Figure 1. Detail perspective views in the area of the cannula injection are also provided for a better demonstration of the cannula geometry and position (Fig, 1). For the antegrade perfusion, the inlet boundary is at the cannula as indicated by arrows (Fig. 1). The main flow direction is also indicated by an arrow. For the physiological circulation, there is no cannula inserted, and the inlet boundary is at the upstream end of the aorta, which is positioned at somewhat downstream from the heat valve, and which is defined to be an impermeable wall for the case of antegrade perfusion (clamped under operation conditions). In Figure 1, the labeling of aortic branches is also indicated, which will be used for defining boundary conditions.

In generating the grids, an unstructured strategy is applied, where tetrahedral and hexahedral cells are used in combination. A formal grid independency study, specific to the present is not performed, where we rely rather on the previous experience [11,16] on the required grid resolution. Since similar grid resolutions are used in both cases, and since the present study aims a comparison between the two computations (without e.g. comparison with measurements), we are quite confident that the comparative assessments will still be meaningful. The generated grids (Figure 2) have approximately 350,000 cells.

Mathematical and Numerical Modelling

Three-dimensional, steady-state and pulsatile flows are analyzed. The wall distensibility is neglected, as this does anyhow not play an important role for the steady-state flow, which is the flow mode for the focal point of the present study, i.e. for the extracorporeal circulation. Shear stresses in large arteries are typically sufficiently large to assume that blood behaves as a Newtonian fluid [17]. Thus, blood is assumed to be a Newtonian fluid for the present purposes, and the Navier-Stokes equations with constant material properties are solved.

Depending on the geometry and the flow mode (physiological vs. extracorporeal, or steady-state vs. pulsatile) the local and temporal Reynolds numbers vary, and since these variations are probably taking place around a critical value, the flow turbulence can be affected by them, calling for an adequate turbulence modeling approach. For example, for the physiological flow, the Reynolds number (Re) at the inlet of Aorta-1, i.e. at the boundary downstream the aortic valve was about 1150, based on the local diameter and the time-averaged

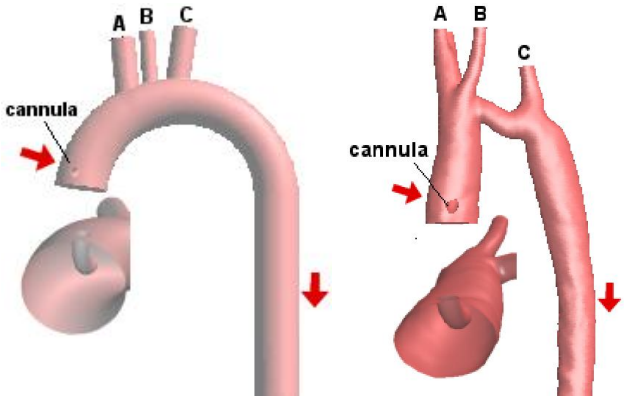

Figure 1 Geometries, Left: Aorta-1, Right: Aorta-2

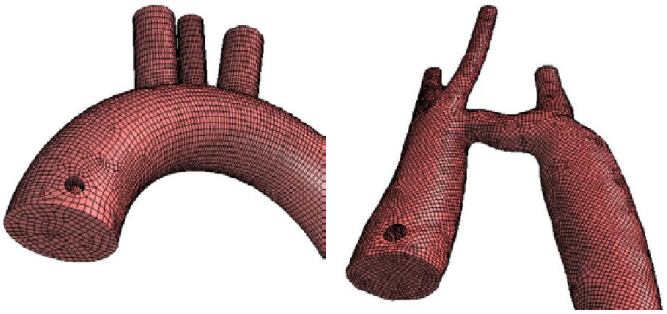

Figure 2 Grids, Left: Aorta-1, Right: Aorta-2

bulk velocity. On the other hand, for the antegrade perfusion, the inlet Reynolds number (Re at the cannula outlet) was much higher, i.e. about 6000. It is generally accepted that the transition from laminar to turbulent flow typically occurs around Re = 2300 for a pipe flow (whereby it is also known that this value has a rather indicative role, and turbulence onset can occur at different Re, depending on flow conditions). Thus, one can imagine that transitional effects can play a role, in such flows. A fairly laminar flow throughout the aorta may rather be expected for the physiological flow, although local effects causing local turbulence generation in the downstream may not be precluded a priori (and except the temporal effects where the flow rate reaches the peak value, but rather for a short time of the pulse). For the antegrade perfusion, the inlet Re indicates a rather turbulent flow, which may re-laminarize in the downstream. For optimally coping with the situation, the flow was modelled as turbulent via the so-called "Shear Stress Transport" model [18], which is a two-equation model that can principally accommodate for some transitional effects.

The governing equations are discretized by a colocated finite volume method, using the SIMPLEC algorithm for treating the velocity-pressure coupling for steady-state computations and PISO algorithm for unsteady computations, and employing the Power Law for the discretization of convective terms [19]. In unsteady computations, a second-order implicit time discretization is used [19]. Time-step sizes are chosen in such a way that the maximum cell Courant numbers [19] remain below unity. In the unsteady simulations, the flow is computed, first, for a period of several pulses, until a fully periodic flow is achieved. Thereafter, time-averaging is performed. Doing so, an eventual influence of (rather arbitrary) initial conditions on the unsteady results and on their time-average is prevented.

Boundary Conditions

For the physiological circulation, the inlet boundary is nearly at the position of the heart valve. For the antegrade perfusion, the inlet boundary is placed at the geometric outlet of the cannula (where the inlet boundary of the physiological circulation is declared to be a wall, in this case). At inlets, for all cases, spatially uniform distributions are prescribed for all variables, assuming the velocity being normal to the boundary. For all cases, the inlet boundary conditions of the turbulence quantities are derived assuming a local turbulence intensity and a length scale. For the turbulence intensity, low values are prescribed (0.1/%) if the inlet Reynolds number is indicating a theoretically laminar flow. Otherwise, a turbulence intensity of 4% is prescribed. The macro length scale is always assumed to be 30% of the inlet (hydraulic) diameter.

For the pulsatile computation of the physiological circulation, the pulse form reported in [20] at a further downstream position of the aortic valve (at the position of the carotid artery) is used, which is slightly different from that reported [19] at the position of the heart valve. Doing so, it is assumed that the shift in the pulse form between the two positions is mainly caused by the distensibility of the aorta walls, as such effects play a role especially in the initial regions of the aorta. Since the wall distensibility is not modelled in the present study, this pulse form [20] is assumed to be more representative for the present modelling of the flow in the whole aorta domain. Nevertheless, differences between the both pulse shapes may be considered to play a rather secondary role for the present analysis, since the extracorporeal circulation (antegrade perfusion) is in the foreground, where the flow is steady-state and the wall-distensibility effects are, thus, less important compared to the pulsatile, physiological circulation.

In defining the solution domain, the considered aorta branches need to be cut at one place, resulting in "outlet" boundaries that require a convenient formulation. It is obvious that such boundary conditions cannot readily be formulated. However, it is also obvious that their appropriate formulation is decisive for the flow distribution between the different branches. For the physiological circulation, empirical values exist for a "normal" percentage distribution [21]. For example, the distribution given in Table I may quite reliably be assumed for the branches shown in Figure 1, for the physiological circulation. Nevertheless, for anatomies largely differing from the "normal" one, and for different perfusion techniques used in extracorporeal circulation, it is difficult to assume that this distribution (Table I) remains valid. An alternative approach could be the prescription of the static pressure at outlets (the same value at all outlets). However, as also discussed in the previous work [11,22], this boundary condition, although it may work reasonably well in some cases, is not reliable, in general. As alternative, an outlet boundary condition based on loss-coefficients was proposed by present authors [11,22]. This boundary condition will mainly be used in the present study, by also making comparisons with the alternative formulations.

RESULTS

Pulsatile vs. Steady-State Flow

For the physiological circulation, the predicted contours of time-averaged dimensionless speed (nondimensionalized by the inlet value) are displayed in Figure 3, for pulsatile and steady-state flow in planes cutting through the aorta and its branches, for Aorta-2. In these computations, the distribution of Table I is used as boundary condition at branch outlets. One can see that the time-averaged solution of the pulsatile flow and the steady-state solution are practically identical (maximum values differ by 2%) and the latter can be considered to reliably represent the time-averaged flow field. Both results show a narrow high velocity region just before branch C, which is neighboured by rather large recirculation zones in the entry region of branch C, and especially on the inner surface of the aortic arch. This is mainly caused by the buckling of the aortic arch after branches A and B (in comparison to the smooth shape of the "normal" Aorta-1). Further recirculation (or low speed) zones are observed, e.g. in the entry region of branch A, or in the descending Aorta. In general, a quite unfavourable velocity distribution is observed for Aorta-2.

Comparison of Different Boundary Condition Formulations

Predicted (steady-state) dimensionless velocity fields for the

Table I. Percentage distribution of total flow rate among the branches A, B, C (Fig. 1).

Branch	A	B	C
% Flow Rate	15	7.5	7.5

physiological circulation by prescribing different boundary conditions, i.e. by prescribing the static pressure (the same value everywhere), and, alternatively, loss-coefficients (as described in [11,22]) at the outlet boundaries, are displayed in Figure 4. In combination with Figure 3, the influence of using different boundary conditions can be observed. The qualitative flow patterns obtained by prescribing loss-coefficients (Fig. 4a) or the static pressure (Fig. 4b) are similar to those obtained by prescribing an outlet flow rate distribution. There are, though, considerable quantitative differences, such as the maximum velocity being approx. 30% lower for the loss-coefficient formulation (Fig. 4a) and approx. 60% lower for the pressure formulation (Fig. 4b) compared to the prescribed outlet mass flow rate (Fig. 3b). In flow fields shown in Figure 4, the flow rates through branches A and B are stronger (especially for Fig. 4b), in comparison to Figure 3. As different boundary conditions produce different results, relying on previous experience [11,22], we assume that the loss-coefficient formulation is the one that can be used most universally, and this formulation will be used in the remainder of the paper, for all cases (since a comparative study between two computations is done, the right choice of the boundary conditions may also be seen to be less critical compared to a case where predictions should be compared with measurements)

Physiological Circulation

For the physiological circulation, the predicted (steady-state) distributions of speed in planes cutting through the aorta and branches are illustrated in Figure 5, for Aorta-1 and Aorta-2. Since Aorta-2 has a smaller inlet area, with the same flow rate, the inlet speed of Aorta-2 is higher (about 50%) than that of Aorta-1. One can observe that the speed distribution remains comparably homogeneous for Aorta-1, where a quite inhomogeneous distribution is obtained for Aorta-2, especially in the region between branches B and C. In this region (Aorta-2), much higher velocity values are attained in comparison to Aorta-1. Predicted turbulence kinetic energies are displayed in the same planes for Aorta-1 and Aorta-2, in Figure 6. At the inlets the turbulence kinetic energies are similarly low, for Aorta-1 and Aorta-2. As the turbulence kinetic energy remains low in downstream, for Aorta-1, a considerable production of turbulence kinetic energy is observed for Aorta-2. The turbulence is mainly generated by the sharp velocity gradients associated with the large recirculation zone caused by the buckled aortic arch in the region between branches B and C. Figure 7 displays the predicted distributions of the wall shear stress for Aorta-1 and Aorta-2. One can see that very much higher shear stress values are predicted for Aorta-2, compared to Aorta-1. The most critical region is, again, the part of the arch between branches B and C. In general, quite large differences in the flow fields of Aorta-1 and Aorta-2 are observed, for the physiological circulation. Aorta-2 exhibits a much more inhomogeneous flow field, much higher velocities, turbulence levels and wall shear stresses.

Extracorporeal Circulation via Antegrade Perfusion

For extracorporeal circulation via antegrade perfusion, the predicted (steady-state) distributions of speed in planes cutting through the aorta and branches are illustrated in Figure 8, for

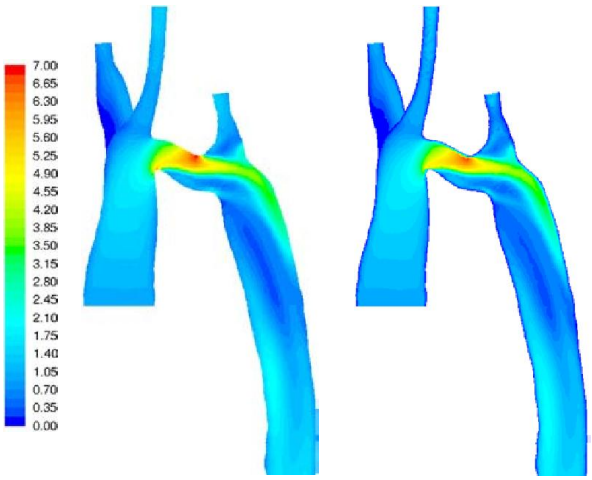

Figure 3 Time-averaged dimensionless speed for physiologic circulation in Aorta-2, Left: pulsatile, Right: steady-state

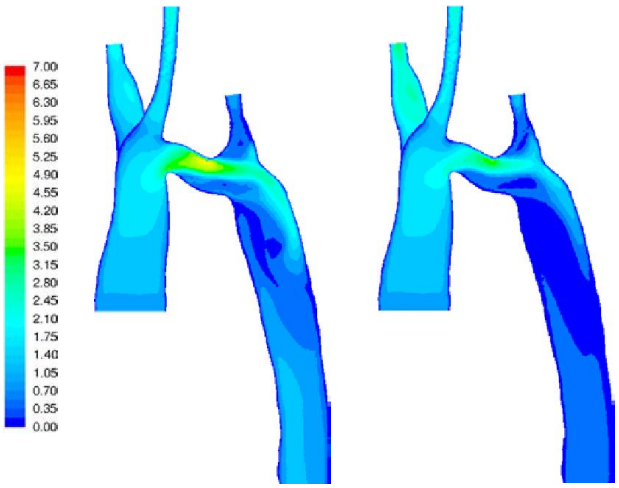

Figure 4 Dimensionless speed for physiologic circulation in Aorta-2 (steady-state), Left: loss-coefficient, Right: pressure

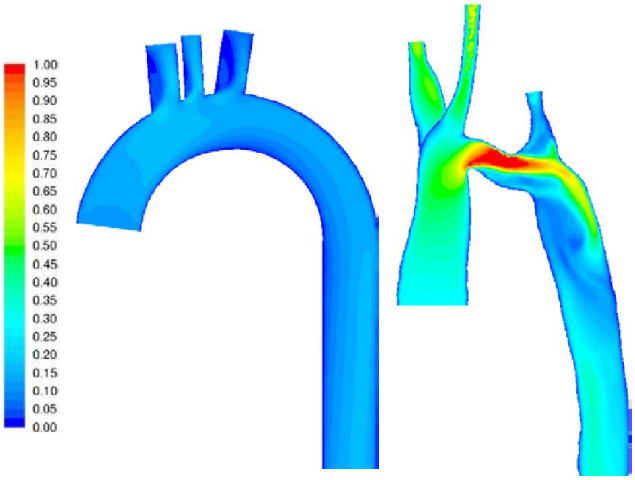

Figure 5 Speed (m/s) for physiological circulation, Left: Aorta-1, Right: Aorta-2.

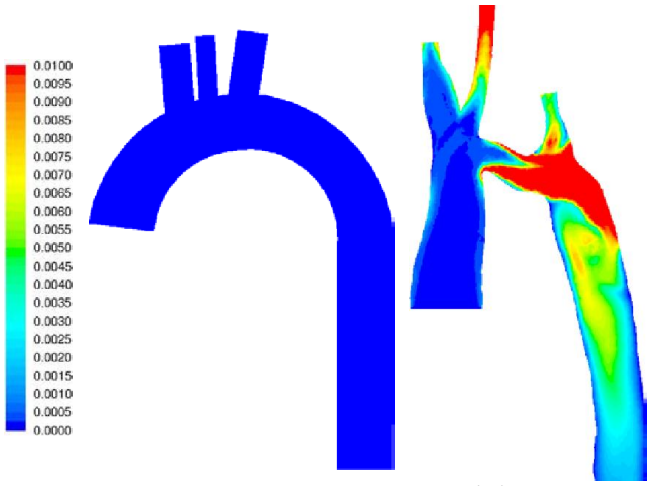

Figure 6 Turbulence kinetic energy (m^2/s^2) for physiological circulation, Left: Aorta-1, Right: Aorta-2

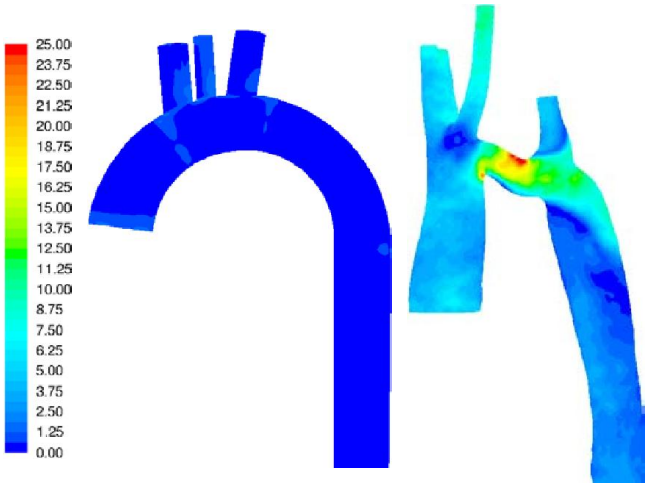

Figure 7 Wall shear stress (Pa) for physiological circulation, Left: Aorta-1, Right: Aorta-2.

Aorta-1 and Aorta-2. Please note that the flow rates, here, are smaller compared to the physiological circulation (the flow rate of the antegrade perfusion is prescribed to be 80% of that of the physiological circulation). The maximum velocities occur in the jet caused by the cannula, and are practically the same for both cases (the same cannula geometry and flow rate). For Aorta-2, the flow field in the initial part, i.e. in the region between the cannula and branch A/B is quite complex. There are comparably strong recirculation zones. This is also the reason, why a high velocity region is observed along the side wall of the initial part of the aorta. This region is associated with a recirculation zone with high near-wall velocities. High velocities are also observed in the part between branches B and C (as it was also the case for physiological circulation, Fig. 5). Predicted turbulence kinetic energies are displayed in the same planes for Aorta-1 and Aorta-2, in Figure 9. In antegrade perfusion (Fig. 9), the turbulence levels are much higher compared to the physiological circulation (Fig. 6), due to the high velocities and turbulence introduced by the cannula jet.

The differences in the turbulence levels between Aorta-1 and Aorta-2, in antegrade perfusion (Fig. 9) are also smaller compared to the physiological circulation (Fig. 6). However, it can still be observed that the turbulence generation is greater in Aorta-2 compared to Aorta-1 (Fig. 9). This is mainly due to the rather strong recirculation zones in the initial regions, which was already mentioned in association with Figure 8. Figure 10 illustrates the predicted distributions of the wall shear stress for Aorta-1 and Aorta-2. It is interesting to note that the maximum values predicted for Aorta-2 are similar between physiological circulation (Fig. 7) and antegrade perfusion (Fig. 10). In antegrade perfusion, similar maximum values are also obtained for Aorta-1 and Aorta-2 (Fig. 10). One can, however, see that the amount of area subject to high wall shear stress is much larger for Aorta-2, compared to Aorta.-1 (Fig. 10).

For antegrade perfusion, in general, the maximum values obtained for velocities, turbulence intensities and walls shear stresses are similar for Aorta-1 and Aorta-2. However, one can still observe that the flow field of Aorta-2 exhibits a higher degree of inhomogeneity. The highly turbulent flow regions are larger, and larger regions of aorta walls are subject to high wall shear stresses. This implies a higher risk of thrombus formation and mobilisation of arteriosclerotic plaques for Aorta-2.

CONCLUSIONS

Based on the present study, the following conclusions can be drawn:

- If the time-averaged flow field is of interest, the steady-state predictions can be used, as both solutions are very similar.
- The formulation used for the outlet boundary conditions has a considerable influence on the results. Presently, a loss-coefficient based formulation is preferred, as a more generally applicable one. A deeper investigation of this issue will be considered in the future work.
- For the physiological circulation, the flow fields of Aorta-1 and Aorta-2 show remarkable differences, where the flow structure observed for Aorta-2 is quite unfavorable. A critical issue seems to be the overloading of the piece of aortic arch between branches B and C.

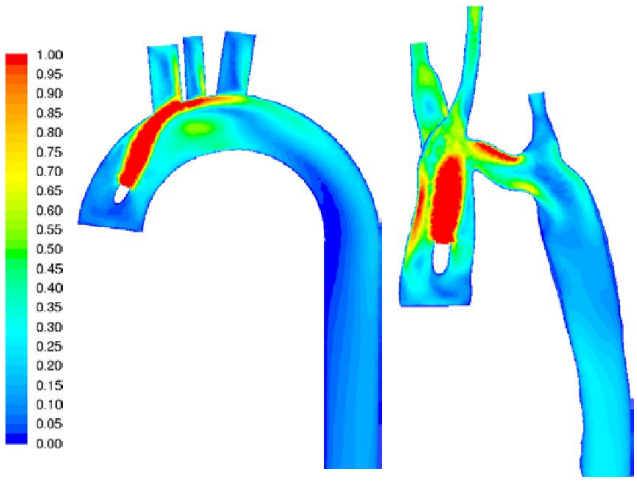

Figure 8 Speed (m/s) for antegrade perfusion, Left: Aorta-1, Right: Aorta-2.

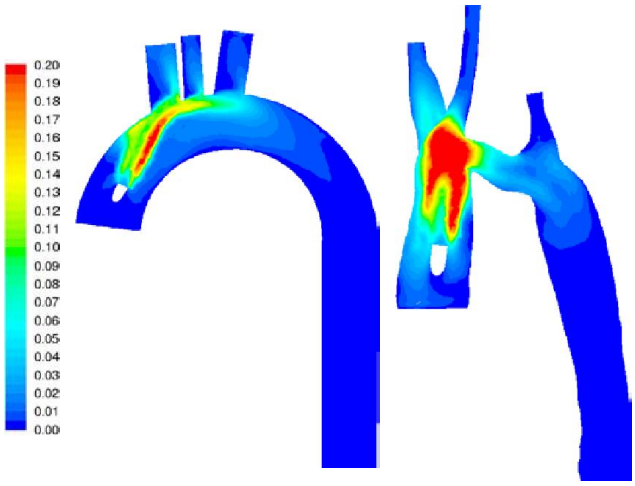

Figure 9 Turbulence kinetic energy (m^2/s^2) for antegrade perfusion, Left: Aorta-1, Right: Aorta-2

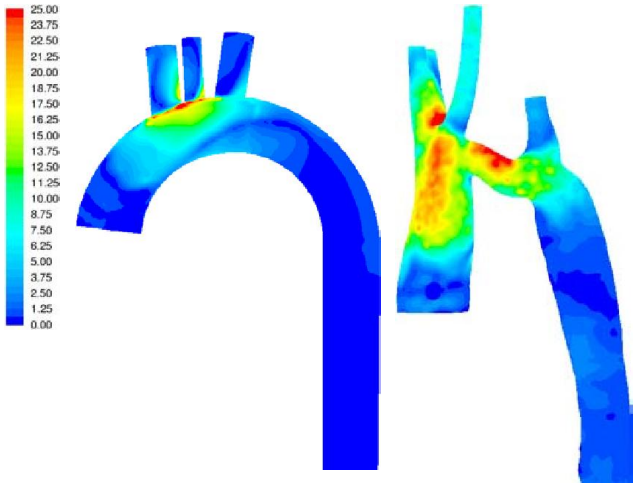

Figure 10 Wall shear stress (Pa) for antegrade perfusion, Left: Aorta-1, Right: Aorta-2

• It is demonstrated that the consequences of the antegrade perfusion for an abnormal and idealized/normal aorta turn out to be different, depending on the details of the specific aorta physiology. For Aorta-2 higher risks for thrombus formation and aretriosclerotic plaque mobilization are observed.

• This comparison indicates that it is advisable to perform a patient-specific detailed computational analysis in advance, for the patients with abnormal physiology, instead of assuming a usual/normal behavior for extracorporeal circulation.

REFERENCES

[1] Mazumdar J. N., Biofluid Mechanics, World Scientific, Singapore, 1992.

[2] Bertram, C. and Gaver III, D. P., Biofluid mechanics of the pulmonary system, *Annals of Biomedical Engineering*, Vol. 33, 2005, pp. 1681-1688.

[3] Pedrizetti, G., and Perktold, K. (Eds.), Cardiovascular Fluid Mechanics, Springer, Wien, 2003.

[4] Mora, C. T., Guyton, R. A., Finlayson, D. C. and Rigatti, R. L. (Eds.), Cardiopulmonary Bypass: Principles and Techniques of Extracorporeal Circulation, Springer, Berlin, 1995.

[5] Yokoyama, Y., Medart, D., Hormes, M., Schmitz, C., Hamilton, K., Kwant, P. B., Takatani, S., Schmitz-Rode, T. and Steinseifer, U., CFD simulation of a novel bileaflet mechanical heart valve prosthesis: an estimation of the Venturi passage formed by the leaflets, *International Journal of Artificial Organs*, Vol. 29, 2006, pp. 1132-1139.

[6] Li, H.-D. and Chan, W. K., Inverse design and CFD investigation of blood pump impeller, *Critical Reviews in Biomedical Engineering*, Vol. 28, 2000, pp. 75-80.

[7] Wood, N. B., Weston, S. J. Kilner, P. J., Gosman, A. D. and Firmin, D. N., Combined MR imaging and CFD simulation in the human descending aorta, *Journal of Magnetic Resonance Imaging*, Vol. 13, 2001, pp. 699-713.

[8] Lee, D. and Chen, J. Y., Numerical simulation of steady flow fields in a model of abdominal aorta with its peripheral branches, *Journal of Biomechanics*, Vol. 35, 2002, pp. 1115-1122.

[9] Tokuda, Y., Song, M. H., Ueda, Y., Usui, A., Akita, T., Yoneyama, S. and Maruyama, S., Three-dimensional numerical simulation of blood flow in the aortic arch during cardiopulmonary bypass, European Journal of Cardio-Thoracic Surgery, Vol. 33, 2008, pp. 164-167.

[10] Minakawa, M., Fukuda, I., Inamura, T., Yanaoka, H, Fukui, K., Daitoku, K, Suzuki, Y. and Hashimoto, Y., Hydrodynamic evaluation of axillary artery perfusion for normal and diseased aorta. General Thoracic and Cardiovascular Surgery, Vol. 56, 2008, pp. 215-221.

[11] Assmann, A., Benim, A. C., Nahavandi, A., Turan, E., Schubert, D., Gams, E. and Feindt, P. Aortic blood flow characteristics of different extracorporeal circulation techniques during cardiac surgery - a computational fluid dynamics approach, *IFMBE Proceedings 25/IV*, Springer, Berlin, 2009, pp. 1604-1607.

[12] http://dicom.nema.org.

[13] Vikal, S., Thainual, P. U., Carrino, J. A., Iordachita, I., G., Fischer, G. S. and Fichtinger, G. Perk station – percutaneous surgery training and performance measurement station, *Computerized Medical Imaging and Graphics*, Available online, doi: 10.1016/j.compmedimag.2009-05.001, 2009.

[14] Papademetris, X., Jackowski, M., Rajeevan, N., Constable, R. T. and Staib, L. H., Bioimage Suite User's Manual", www.bioimagesuite.org , 2008.

[15] Ansys Fluent 12.0, User's Guide, Fluent Inc., Lebanon, NH, USA , 2009.

[16] Khorrami, P. (2009) Numerische Analyse der Blutströmung im menschlichen Körper, M.Sc. Thesis, Duesseldorf University of Applied Sciences, Germany.

[17] Pedley T. J. (2003) Arterial and venous fluid dynamics, in: Pedrizetti G., and Prektold K. (Eds.) *Cardiovascular Fluid Dynamics*, Springer, Wien, 2003, pp 73-136.

[18] Menter, F. R. (1993) Zonal two equation k-ω turbulence models for aerodynamic flows, *AIAA Paper 93-2906*.

[19] Peyret, R. (1996) *Handbook of Computational Fluid Mechanics*, Academic Press, San Diego.

[20] van de Vosse, F. N. (1987) Numerical Analysis of Carotid Artery Flow, Dissertation, Technical University of Eindhoven.

[21] Middleman, S. (1972) Transport Phenomena in Cardiovascular System, John Wiley & Sons.

[22] Benim, A. C., Nahavandi, A., Assmann, A., Schubert, D., Feindt, P. and Suh, S. H. (2009) Simulation of flow in human aorta with emphasis on outlet boundary conditions, *Applied Mathematical Modelling* (submitted).